

FIG. 3. Superbanana orbit of a particle trapped in a localized magnetic well in the stellarator.

the well boundary prevented the periodic motion necessary for the conservation of the action.

The existence of the stellarator superbananas corresponds to the localization of the magnetic wells  $B = W/\mu$ . Furthermore, the remainder of the stellarator magnetic wells, which are not localized, produced no superbananas. No superbananas were found in the torsatron configuration, for which no localized magnetic wells exist.

From this work, we have found the following conclusions valid for single-charged-particle

motion in vacuum magnetic fields for the classical stellarator and torsatron:

(1) Action is not conserved in classical stellarators and torsatrons.

(2) Superbananas are a property of the magnetic well topology of the stellarator, and appear on the exterior of the torus only.

(3) Superbananas do not appear in the classical torsatron.

This work was supported by the U. S. Department of Energy under Contract No. ET-78-S-02-5069 and the National Science Foundation under Grant No. ENG-77-14820.

<sup>1</sup>C. Gourdon, D. Marty, E. K. Maschke, and J. P. Dumont, in *Proceedings of the Third International Conference on Plasma Physics and Controlled Nuclear Fusion Research, Novosibirsk, U. S. S. R., 1968* (International Atomic Energy Agency, Vienna, Austria, 1969), Vol. I, p. 847.

<sup>2</sup>A. Gibson and J. B. Taylor, *Phys. Fluids* **10**, 2653 (1967).

<sup>3</sup>A. Gibson and D. W. Mason, *Plasma Phys.* **11**, 121 (1969).

<sup>4</sup>A. A. Galeev, R. Z. Sagdeev, H. P. Furth, and M. N. Rosenbluth, *Phys. Rev. Lett.* **22**, 511 (1969).

<sup>5</sup>K. Miyamoto, *Nucl. Fusion* **18**, 2, 243 (1978).

<sup>6</sup>H. P. Furth and M. N. Rosenbluth, in *Proceedings of the Third International Conference on Plasma Physics and Controlled Nuclear Fusion Research, Novosibirsk, U. S. S. R., 1968* (International Atomic Energy Agency, Vienna, Austria, 1969), Vol. I, P. 821.

## Pressure-Jump Studies in Supercritical Mixtures

Ning-Chih Wong and Charles M. Knobler

*Department of Chemistry, University of California, Los Angeles, Los Angeles, California 90024*

(Received 14 September 1979)

Pressure jump experiments have been performed to study the relaxation of isobutyric acid and water mixtures to equilibrium states in the one-phase region near a critical point. Small-angle light-scattering measurements have been used to monitor the approach to equilibrium. The observed time dependence of the scattered intensity is in good agreement with a model proposed by Binder.

Although recent theoretical<sup>1</sup> and experimental<sup>2</sup> investigations of the nonequilibrium behavior of mixtures near a critical point have focused on the processes involved in phase separation, the dynamical behavior of systems that relax to states in a one-phase region of the phase diagram is of interest as well. Binder<sup>1</sup> has used the Kawasaki spin-exchange model to derive a kinetic

equation for the structure factor  $S(k, t)$  in binary mixtures with conserved order parameter. For a temperature jump within the one-phase region from  $T$  to  $T'$  he finds, in the hydrodynamic limit ( $k \rightarrow 0$ ,  $t \rightarrow \infty$ ),

$$S(k, t) = S_T(k) \exp[-D_{T'}(k)k^2t] + S_{T'}(k) \{1 - \exp[-D_{T'}(k)k^2t]\}, \quad (1)$$

where  $k$  is the wave number,  $t$  is the time after the jump,  $S_T(k)$  and  $S_{T'}(k)$  are the equilibrium structure factors at the initial and final temperatures, respectively, and  $D_{T'}(k)$  is the mutual diffusion coefficient at the final temperature.

In the neighborhood of the critical solution temperature  $T_c$ , for a liquid mixture of critical composition, the usual power-law expressions can be used for  $D$  and the correlation length  $\xi$ :

$$D = D_0 \epsilon^\nu g(k\xi),$$

$$\xi = \xi_0 \epsilon^{-\nu};$$

and the equilibrium structure factor can be represented by the Ornstein-Zernike expression

$$S(k) = \Gamma \epsilon^{-\gamma} / (1 + k^2 \xi^2).$$

To demonstrate the evolution of the light-scattering pattern after a quench, these relations and the Kawasaki form<sup>3</sup> of the correlation scaling function  $g(k\xi)$  have been substituted in (1) and the scaled structure factor  $\mathcal{S}(k\xi, \tau) = S(k, t) \epsilon^\gamma / \Gamma$  has been calculated at several scaled times  $\tau = D_0 \epsilon^{3\nu} t / \xi_0^2$  after jumps from  $T = (1 + 2 \times 10^{-4}) T_c$  to  $T' = (1 + 3 \times 10^{-5}) T_c$  and from  $T'$  to  $T$ . For  $T'$  to  $T$ ,  $\mathcal{S}$  undergoes a simple decay [Fig. 1(a)], but for  $T$

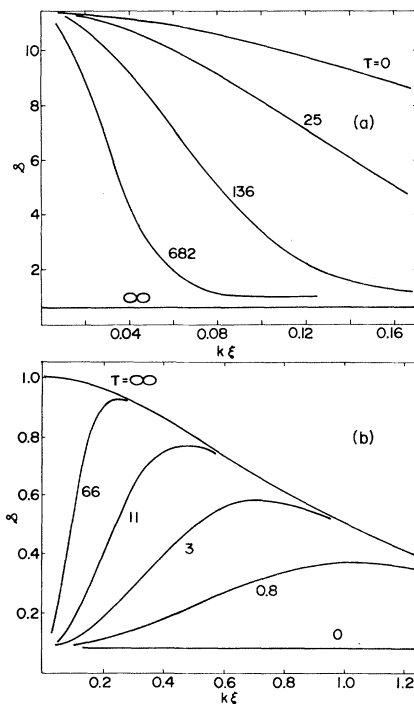


FIG. 1. Evolution of scaled structure factors  $\mathcal{S}(k\xi, \tau)$  calculated in accordance with Eq. (1). (a) Jump from  $T' = (1 + 3 \times 10^{-5}) T_c$  to  $T = (1 + 2 \times 10^{-4}) T_c$ . (b) Jump from  $T = (1 + 2 \times 10^{-4}) T_c$  to  $T' = (1 + 3 \times 10^{-5}) T_c$ .

to  $T'$  [Fig. 1(b)],  $\mathcal{S}$  displays a maximum that moves toward smaller angle with increasing  $\tau$ . Such behavior was observed<sup>4</sup> in Monte Carlo simulations of quenches in solid binary mixtures from  $T = \infty$  to  $T' = 1.1 T_c$ . We have undertaken studies of liquid mixtures to determine if the relaxation above  $T_c$  can also be adequately described by Eq. (1).

The experimental method and procedures were similar to those previously described.<sup>2</sup> Scans of the scattered intensity from isobutyric acid + water mixtures at angles from about 3 to 13 deg were accomplished in 10 ms by rotating the scanning mirror at 300 rpm. Precautions were taken to reduce light scattered in the forward direction by dust and by windows. The detection system was designed to make the scattering volume essentially independent of scattering angle and this feature was confirmed by measurements of the fluorescence of a fluorescein solution. Further checks of the performance of the apparatus were measurements of the equilibrium scattering at small angles ( $1.6^\circ - 11^\circ$ ) at temperatures from 2 to 5 mK above  $T_c$ , which are well represented by the Ornstein-Zernike expression and give values

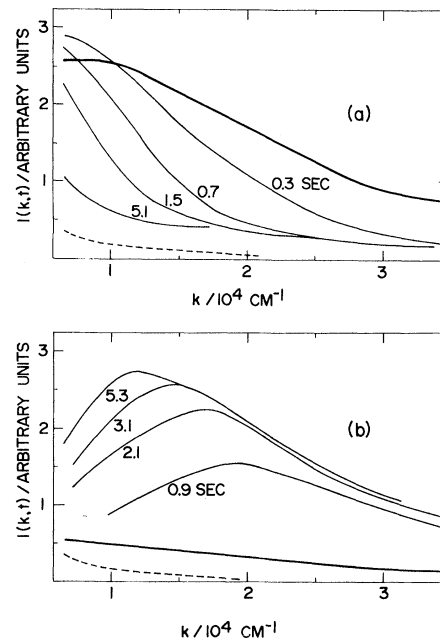


FIG. 2. Measured intensity profiles at various times after a pressure jump of 1 atm. Full lines represent intensity profiles just before the pressure quench. Dashed lines represent intensity profiles at about  $T_c + 10$  K and are used as background corrections. (a) Jump from  $T' = T_c + 10$  mK to  $T = T_c + 70$  mK. (b) Jump from  $T = T_c + 70$  mK to  $T' = T_c + 10$  mK.

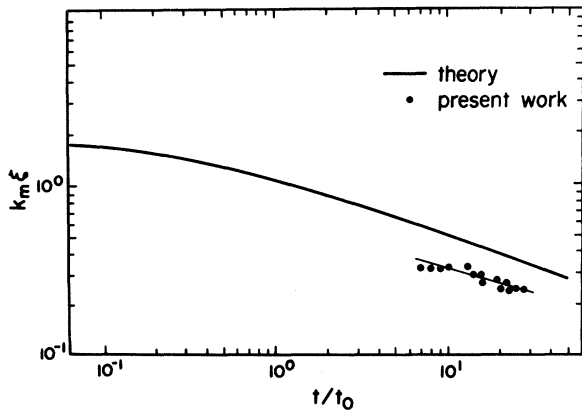


FIG. 3. Reduced-scale plot of position of maximum intensity vs time:  $q_m = k_m \xi$  and  $\tau = t/t_0$ . The solid line is calculated in accordance with Eq. (1).

of  $\xi$  consistent with those reported by Chu, Lee, and Tscharnuter.<sup>5</sup> These studies also confirm that for the geometry employed the effect of multiple scattering is small at low angles.<sup>6</sup> In the neighborhood of the maxima, the scatter in the relative intensity is 5%.

Figure 2 shows the scattered intensity as a function of  $k$  and  $t$  for two jump experiments nominally equivalent to those for which the curves in Fig. 1 were computed. In Fig. 2(a) the system was equilibrated at  $T_c + 10$  mK and then brought to  $T_c + 70$  mK by a 1-atm increase in the applied pressure. Such a change is essentially adiabatic since the thermal time constant of the sample

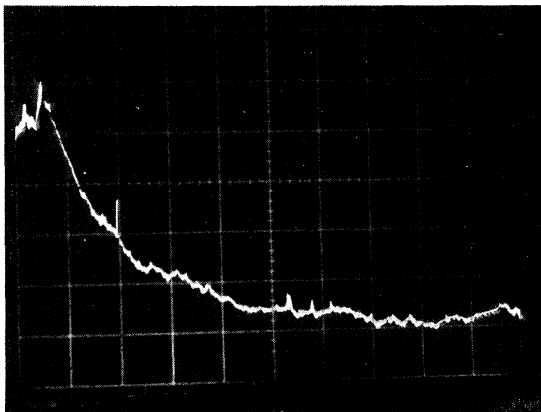


FIG. 4. Oscillogram of the scattered intensity at fixed angle ( $5^\circ$ ) after a pressure quench of 1 atm. Temperature of the system is equilibrated at 10 mK above  $T_c$  prior to the pressure quench. The horizontal sweep speed is set at 0.2 s/div. A spike can be seen at the onset of the intensity drop.

( $\sim 1$  min) is much longer than the duration of a typical measurement. As a result, the jump is about 5 mK larger than its nominal value. Similarly, the final temperature in the jump shown in Fig. 2(b) was about 5 mK rather than 10 mK because of the adiabatic cooling accompanying the pressure release.

A comparison between the corresponding curves in Figs. 1 and 2 shows that Eq. (1) provides a qualitatively correct representation of the experimental results. Over the relatively small time interval ( $1 \text{ s} < t < 10 \text{ s}$ ) that the position of the maximum in the scattering,  $k_m$ , can be followed we find  $k_m \propto t^{-0.3}$ . When values of  $D$  and  $\xi$  taken from light-scattering measurements<sup>5</sup> are used in Eq. (1), the maximum in the calculated curves decreases as  $t^{-0.33}$  but the values of  $k_m$  are about 50% larger in magnitude than those observed (Fig. 3). It should be noted, however, that there are no adjustable parameters in this calculation and that uncertainties of 1 mK in  $T$  or 0.01 in  $\nu$  can produce (20–30)% shifts in the time scale that are sufficient to bring experiment and theory into excellent agreement.

A test of the consistency of experiment and

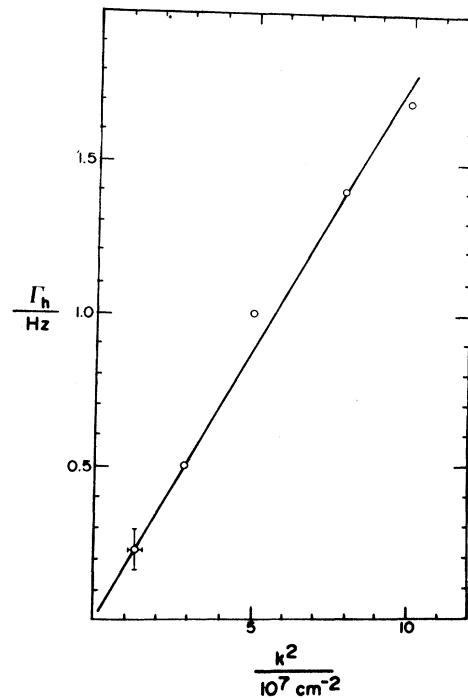


FIG. 5. Plot of inverse of decay time  $\Gamma_h$  vs  $k^2$  at five scattering angles following a jump from  $T_c + 10$  mK to  $T_c + 70$  mK. The slope yields the mutual diffusion coefficient:  $D = 1.7 \times 10^{-8} \text{ cm}^2 \text{ s}^{-1}$ .

theory is provided by measurements of the intensity as a function of time at fixed angle. Under such conditions Eq. (1) predicts an exponential change in  $S$  with a time constant  $t_0 = 1/Dg(k\xi)k^2$ , whose inverse should be equivalent to the line-width observed from the decay of spontaneous fluctuations by light-beating spectroscopy. In essence, the jump experiments prepare the system in a well-defined nonequilibrium state and allow a classical measurement of the relaxation to equilibrium to be performed.

Values of  $t_0$  were obtained by recording with a storage oscilloscope the decrease in intensity at a fixed angle between  $2^\circ$  and  $8^\circ$  following a jump from  $T_c + 10$  mK to  $T_c + 70$  mK (Fig. 4). The width of the trace at  $e^{-1}$  of the peak intensity is taken as  $t_0$  and its inverse  $t_0^{-1} = \Gamma_h$  is plotted against  $k^2$  in Fig. 5. At these angles  $g(k\xi) \approx 1$ , and hence the slope of line gives directly  $D = 1.7 \times 10^{-8} \text{ cm}^2 \text{ s}^{-1}$ , in good agreement with the value  $D = 1.6 \times 10^{-8} \text{ cm}^2 \text{ s}^{-1}$  at  $T_c + 70$  mK calculated from the light-beating results.<sup>5</sup>

An interesting detail of Fig. 4 is the spike that appears immediately after the pressure jump. In jumps from high to low temperatures a corresponding dip is observed. The spike and dip decrease in size with increasing scattering angle. These features are the result of the contributions

to the turbidity of fluctuations that scatter at angles considerably higher than those at which our measurements are performed. On the time scale of our experiment, these fluctuations reach equilibrium instantaneously and produce a step change in the turbidity that is seen as a steep rise (or fall) in the scattering. Calculations of the turbidity as a function of time by integration of Eq. (1) reproduce in detail all of the observed phenomena. These results are consistent with models in which cluster dynamics are assumed to occur by diffusion of large clusters in a fluid containing an equilibrium distribution of small clusters.

This work was supported by the National Science Foundation.

<sup>1</sup>K. Binder, Phys. Rev. B **15**, 4425 (1977).

<sup>2</sup>N. C. Wong and C. M. Knobler, J. Chem. Phys. **69**, 725 (1978).

<sup>3</sup>B. Chu, *Laser Light Scattering* (Academic, New York, 1974), p. 294.

<sup>4</sup>J. Marro, A. B. Bortz, M. M. Kalos, and J. L. Lebowitz, Phys. Rev. B **12**, 2000 (1975).

<sup>5</sup>B. Chu, S. P. Lee, and W. Tscharnuter, Phys. Rev. A **7**, 353 (1973).

<sup>6</sup>H. M. J. Boots, D. Bedeaux, and P. Mazur, Physica (Utrecht) **84A**, 217 (1976).

## Is the Phase Transition of the Three-State Potts Model Continuous in Three Dimensions?

S. J. Knak Jensen and O. G. Mouritsen

*Department of Physical Chemistry, Chemical Institute, Aarhus University, DK-8000 Aarhus C, Denmark*

(Received 24 August 1979)

The internal energy and the order parameter of the three-state Potts model in a simple cubic lattice are calculated using the Monte Carlo technique. Both properties exhibit metastabilities in a small temperature region demonstrating that *the phase transition is of first order*. This result is in agreement with the prediction of the  $\epsilon$  expansion but in contrast to the position-space renormalization-group calculations which lead to a continuous transition.

The  $q$ -state Potts model is a generalization of the standard Ising model in which each lattice site can be in one of  $q$  distinct states,  $\sigma = 1, 2, \dots, q$ . The Hamiltonian of the Potts model may be written as

$$H = -J \sum_{\langle j,k \rangle} (2\delta_{\sigma_j \sigma_k} - 1), \quad (1)$$

where the sum is over nearest-neighbor pairs, and  $J$  is an energy parameter. According to Eq. (1) the interaction between a pair of nearest-neighbor sites is  $-J$  if the sites are in the same

state and  $+J$  if they are in different states. Evidently the standard Ising model corresponds to  $q = 2$ .

In this Letter we shall be concerned with the order of the phase transition of the three-state Potts model in three dimensions, a problem which has been subject to considerable discussion. High-temperature series analyses<sup>1</sup> and exact calculations<sup>2</sup> show that the three-state Potts model has a continuous transition in the two-dimensional case whereas mean-field theory

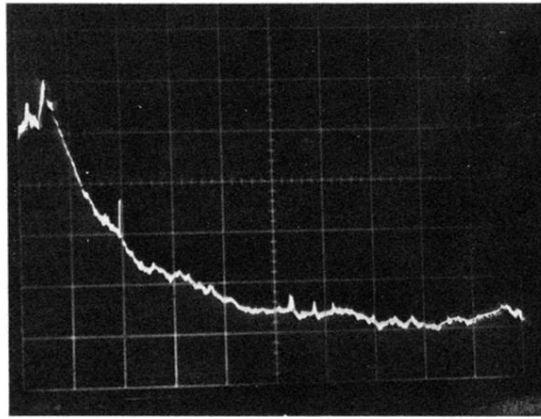


FIG. 4. Oscillogram of the scattered intensity at fixed angle ( $5^\circ$ ) after a pressure quench of 1 atm. Temperature of the system is equilibrated at 10 mK above  $T_c$  prior to the pressure quench. The horizontal sweep speed is set at 0.2 s/div. A spike can be seen at the onset of the intensity drop.